

Spectral analysis of multi mode pulsating sdB stars II. Feige 48, KPD 2109+4401 and PG 1219+534 *

U. Heber¹, I.N. Reid², K. Werner³

¹ Dr.-Remeis-Sternwarte, Universität Erlangen-Nürnberg, Sternwartstr. 7, D-96049 Bamberg, Germany INTERNET: heber@sternwarte.uni-erlangen.de

² Department of Physics and Astronomy, University of Pennsylvania, Philadelphia, PA 19104-6396, USA INTERNET: inr@herschel.physics.upenn.edu

³ Institut für Astronomie und Astrophysik, Universität Tübingen, D-72076 Tübingen, Germany INTERNET: werner@astro.uni-tuebingen.de

received; accepted

Abstract. Three members of the new class of pulsating sdB stars (sdBV or EC 14026 stars) are analysed from Keck HIRES spectra using line blanketed NLTE and LTE model atmospheres. Atmospheric parameters (T_{eff} , $\log g$, $\log(\text{He}/\text{H})$), metal abundances and rotational velocities are determined. A careful investigation of several temperature indicators, i.e. line profile fitting of Balmer and helium lines, the ionization equilibria of helium, nitrogen and silicon gave consistent results for Feige 48 and KPD2109+4401 to within a few hundred Kelvin. However, for PG 1219+534 considerably higher effective temperature estimates were derived from the ionization equilibria of nitrogen (36 800 K) and helium (34 400 K) than from the Balmer line profile fitting (33 200 K). A systematic difference in the gravity derived from NLTE and LTE models was observed, the NLTE gravities being slightly lower, by up to 0.1 dex, than the LTE results.

As is typical for sdB stars, all programme stars are found to be helium deficient, with a helium abundance ranging from 1/80 solar for Feige 48 to 1/3 solar for PG 1219+534, probably due to diffusion. Most metals are also depleted. The abundances of C, O, Ne, Mg, Al and Si in the high gravity programme stars KPD 2109+4401 and PG 1219+534 are considerably lower than in the lower gravity stars Feige 48 and PG 1605+072 (Heber et al., 1999) which could be explained by an equilibrium between gravitational settling and radiative levitation. Surprisingly iron is solar to within error limits in all programme stars irrespective of their gravity, confirming predictions from diffusion calculations of Charpinet et al. (1997).

The metal lines are very sharp and allow the microturbulent velocity to be constrained to be lower than 5 km/s (KPD 2109+4401, PG 1219+534). Also the projected rotational velocities have to be very low ($v_{\text{rot}} \sin i < 10$ km/s). For Feige 48 the limits are even tighter ($v_{\text{micro}} \leq 3$ km/s, $v_{\text{rot}} \sin i \leq 5$ km/s).

Send offprint requests to: U. Heber

* Based on observations obtained at the W.M. Keck Observatory, which is operated by the Californian Association for Research in Astronomy for the California Institute of Technology and the University of California

Key words: stars: atmospheres – stars: abundances – stars: subdwarfs – Stars: rotation – stars: oscillations – stars: individual: Feige 48, KPD 2109+4401, PG 1219+534

1. Introduction

It is now well established that the hot subluminous B stars can be identified with models of the extreme Horizontal Branch (EHB, Heber, 1986, Saffer et al. (1994). Their photospheric chemical composition is governed by diffusion processes leading to strong peculiarities (e.g. deficiencies of helium, carbon and silicon in some stars) with strong variations from star to star (for a review see Heber, 1998).

Recently, several sdB stars have been found to be pulsating (termed EC14026 stars after the prototype, see O'Donoghue et al. 1999 for a review), defining a new instability strip in the HR-diagram. The study of these pulsators offers the possibility of applying the tools of asteroseismology to investigate the structure of sdB stars. The existence of pulsating sdB stars was predicted by Charpinet et al. (1996), who uncovered an efficient driving mechanism due to an opacity bump associated with iron ionization in EHB models. However, in order to drive the pulsations, iron needed to be enhanced in the appropriate subphotospheric layers, possibly due to diffusion. Subsequently, Charpinet et al. (1997) confirmed this assumption by detailed diffusion calculations. Even more encouraging was the agreement of the observed and predicted instability strip.

Eighteen pulsating sdB stars are well-studied photometrically (see O'Donoghue et al. 1999 for a review, and Billères et al. 2000, Silvotti et al. 2000 and Østensen et al. 2000 for more recent discoveries). A precise knowledge of effective temperature, gravity, element abundances and rotation is a prerequisite for the asteroseismological investigation.

We selected four EC14026 stars for a detailed quantitative spectral analysis (see Fig. 1): PG 1605+072 was chosen because it has the lowest gravity and, therefore, has probably already evolved beyond the extreme horizontal branch phase.

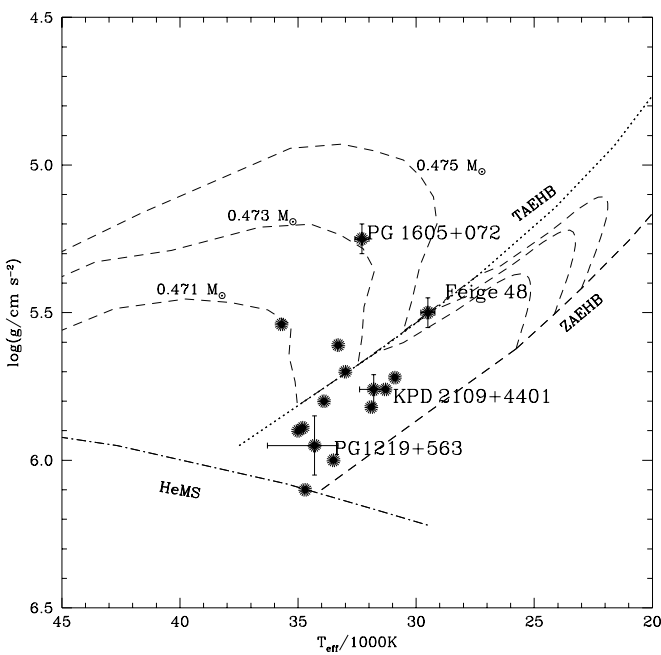


Fig. 1. Position of the programme stars in the (T_{eff} , $\log g$) plane and comparison with other EC 14024 stars which are well-studied photometrically. The position of the zero age extreme Horizontal Branch (ZAEHB), the terminal age extreme Horizontal Branch (TAEHB), the helium main sequence and evolutionary tracks for EHB stars (Dorman et al., 1995) are also shown.

It also displays the richest frequency spectrum amongst the EC 14026 stars (>50 periods have been identified, Kilkenny et al. 1999). The results of a spectral analysis have already been reported by Heber et al. (1999). Recently, Kawaler (1999) predicted from his modelling of the pulsations that PG 1605+072 should be rotating. This prediction was confirmed by the analysis of optical spectra from which a projected rotational velocity of $v_{\text{rot}} \sin i = 39 \text{ km/s}$ was derived (Heber et al., 1999). In this paper we present the spectral analysis of three additional pulsating sdB stars. PG 1219+534 was chosen because it has the shortest pulsation periods and has a helium abundance larger than most other sdB stars (O'Donoghue et al., 1999). Feige 48 was selected because it is the coolest of all EC 14026 stars known (Koen et al., 1998). The effective temperature and gravity of KPD 2109+4401 (Billères et al., 1998) places the star in the parameter space where most EC 14026 stars are found (see Fig. 1). For Feige 48 and KPD 2109+4401 only few frequencies (four for the former, five for the latter) have been found so far.

2. Observations

High resolution optical spectra were obtained with the HIRES echelle spectrograph (Vogt et al. 1994) on the Keck I telescope on July 20, 1998 using the blue cross disperser to cover the full

wavelength region between 3700Å and 5200Å at a resolution 0.09Å.

The spectra are integrated over one pulsation cycle or more since the exposure times (600–900s) were long compared to the pulsational periods.

The standard data reduction as described by Zuckerman & Reid (1998) resulted in spectral orders that have a somewhat wavy continuum. In order to remove the waviness we used the spectrum of H1504+65 (a very hot pre-white dwarf devoid of hydrogen and helium, Werner 1991) which was observed in the same night. Its spectrum has only few weak lines of highly ionized metals in the blue (3600–4480Å) where the strong Balmer lines are found in the sdB stars. Therefore we normalized individual spectral orders 1 to 20 (3600–4480Å) of the sdB stars by dividing through the smoothed spectrum of H1504+65. The remaining orders were normalized by fitting the continuum with spline functions (interpolated for orders 26 and 27 which contain H β). Judged from the match of line profiles in the overlapping parts of neighboring orders this procedure worked extremely well. Atmospheric parameters determined from individual Balmer lines are found to be consistent with each other except for H β . Since this might be a result of interpolation errors in the normalization process, we excluded H β from the fit procedure.

Besides the strong Balmer lines of hydrogen, helium lines are present in all three stars. However, He II 4686Å is detected in KPD 2109+4401 and PG 1219+534, only. In addition, weak photospheric metal lines can be identified in the spectra of all programme stars. However, the number of detectable photospheric lines differs considerably. The largest number of metal lines is present in Feige 48 (C, N, O, Ne, Mg, Si, Al, S and Fe). In PG 1219+534 and KPD 2109+4401 only N, S and Fe are detectable. Also interstellar Ca II lines are present and are found to have a complex structure (three to four components, see appendix).

3. Spectral analysis

The simultaneous fitting of Balmer line profiles by a grid of synthetic spectra has become the standard technique to determine the atmospheric parameters of hot high gravity stars (Bergeron et al. 1992). The procedure has been extended to include helium line profiles as well and applied successfully to sdB stars by Saffer et al. 1994). It will be referred to as Saffer's procedure throughout this paper. The Balmer lines (H γ to H 12), He I (4471Å, 4026Å, 4922Å, 4713Å, 5016Å, 5048Å) and He II 4686Å lines are fitted to derive all three parameters simultaneously.

The analysis is based on an updated version of the LTE model atmosphere code of Heber et al. (1984a) which includes metal line blanketing using Kurucz' ATLAS6 Opacity Distribution Functions. A large grid of models is calculated for various helium abundances and solar metalicity as well as for metal poor ([M/H]=-2.0) composition (see Heber et al. 1999b).

Lemke's version¹ of the LINFOR program (developed originally by Holweger, Steffen, and Steenbock at Kiel University) is used to compute a grid of theoretical spectra which include the Balmer lines H_{α} to H_{22} and He I and He II lines. As can be seen from Tables 1, 3 and 5 the metallicity dependence of the results is marginal, the effective temperature changes by 600 K, the gravity by 0.02 dex and the helium abundance by 0.09 dex at the most when we apply Saffer's procedure with the metal poor LTE grid ($[M/H]=-2.0$) instead of the solar composition grid. Tests using models calculated with Kurucz' ATLAS9 code were also performed. No significant deviations of the fit results from those listed in Table 1 were found.

In order to investigate the role of NLTE effects we repeated the analyses using a grid of H-He line blanketed, metal free NLTE model atmospheres (Napiwotzki 1997), calculated with the ALI code of Werner & Dreizler (1999). Applying Saffer's procedure with the NLTE model grid (see Tables 1, 3 and 5) yields T_{eff} and $\log \frac{n_{\text{He}}}{n_{\text{H}}}$ almost identical to that obtained from the LTE grid. We therefore conclude that the Balmer and helium lines are not vulnerable to NLTE effects.

However, a systematic difference in $\log g$ persists, the LTE values being higher by 0.1 dex than the NLTE results (see Table 1). Since its origin is obscure, we finally adopted the averaged atmospheric parameters given in Tables 1, 3 and 5.

The metal lines are sufficiently isolated to derive abundances from their equivalent widths again using the LINFOR program. Oscillator strengths were taken from the critical compilation of Wiese et al. (1996) for C, N and O, from the Opacity Project (Seaton, 1987) for Ne II, Mg II, and Al III using the Opacity Project data base "TOPbase" (Cunto & Mendoza, 1992) at the CDS (Strasbourg), from Becker & Butler (1990) for Si, Wiese et al. (1969) for S III, and Ekberg (1993) and Kurucz (1992) for Fe III. The oscillator strengths for some lines of light elements which could not be found in the papers cited were supplemented from Kurucz' line list, from which also the damping constants for all metal lines were extracted.

Equivalent widths of metal lines between 5mÅ and 79mÅ were measured. Since fewer metal lines are present in the spectra of KPD 2109+4401 and PG 1219+534 than in those of Feige 48 and PG 1605+072, we use the latter spectra as guidance to determine upper limits for metal abundances of the former from the absence of the presumably strongest lines of the ions in question. An upper limit to their equivalent width of 5mÅ was assumed.

3.1. Feige 48

Since no He II line can be detected, the helium ionization equilibrium can not be evaluated.

The results of the analysis of the H and He I lines for Feige 48 are listed in Table 1 and compared to published values obtained from low resolution spectra. The formal errors of our fits are much smaller than the systematic errors (see below).

¹ For a description see <http://a400.sternwarte.uni-erlangen.de/~ai26/linfit/linfor.html>

Table 1. Atmospheric parameters for Feige 48 from different methods, see text

method	T_{eff} [K]	$\log g$	$\log \frac{n_{\text{He}}}{n_{\text{H}}}$
Koen et al. (1998)	$28\,900 \pm 300$	5.45 ± 0.05	–
LTE: H+He [M/H]=0.0	29 500	5.53	-2.94
LTE: H+He [M/H]=-2.0	30 100	5.53	-2.90
NLTE: H+He	29 600	5.43	-2.93
adopted	$29\,500 \pm 300$	5.5 ± 0.05	-2.93 ± 0.05

Table 2. Metal abundances for Feige 48 compared to solar composition. n is the number of spectral lines per ion.

ion	n	$\log \epsilon$	[M/H]
C III	2	7.36 ± 0.03	-1.27
N II	16	7.47 ± 0.17	-0.48
N III	2	7.80 ± 0.11	-0.15
O II	29	7.79 ± 0.12	-1.09
Ne II	3	7.10 ± 0.31	-0.69
Mg II	1	6.91	-0.6
Al III	2	5.50 ± 0.18	-0.89
Si III	4	6.39 ± 0.32	-1.01
Si IV	1	6.17	-1.07
S III	1	6.15	-1.01
Fe III	26	7.55 ± 0.19	+0.13

The fit of the lines using the NLTE model grid is displayed in Fig. 2. The agreement with the results from low resolution spectra analysed with similar LTE model atmospheres (Koen et al. 1998) is encouraging.

Helium is deficient by a factor of 80 and therefore Feige 48 has the lowest helium abundance among our programme stars.

Three species are represented by two stages of ionization (C II and C III, N II and N III, Si III and Si IV). Since these line ratios are very temperature sensitive at the temperatures in question, we alternatively can derive T_{eff} and abundances by matching these ionization equilibria. Gravity is derived subsequently from the Balmer lines by keeping T_{eff} and $\log \frac{n_{\text{He}}}{n_{\text{H}}}$ fixed. These two steps are iterated until consistency is reached. C II is represented by the 4267Å line only, which is known to give notoriously too low carbon abundances. Indeed the carbon ionization equilibrium can not be matched at any reasonable T_{eff} . The ionization equilibrium of N indicates a slightly higher effective temperature of $T_{\text{eff}} \approx 30\,700$ K than derived from the Balmer and neutral helium lines using Saffer's procedure whereas the silicon ionization equilibrium indicates a slightly lower effective temperature of $T_{\text{eff}} \approx 28\,000$ K. However, in the case of the nitrogen ionization equilibrium, N III is represented by two weak lines only, and in the case of silicon Si IV is represented by one weak line only. Considering the measurement errors for these lines, the nitrogen and silicon ionization equilibria can be considered to be in good agreement with the fit of the Balmer and neutral helium lines.

The effective temperature derived from the metal ionization equilibria is higher than that from Saffer's procedure. Whether this may be caused by an NLTE effect has to be investigated

Fig. 2. Balmer and He line profile fits for Feige 48 of the HIRES spectrum.

from detailed NLTE calculations for N and Si which are beyond the scope of this paper.

Although several O lines are available in the spectrum of Feige 48, it was impossible to determine the microturbulent velocity in the usual way, i.e. by removing the slope of the O abundances with equivalent widths, due to the lack of sufficiently strong lines. However, the spectrum is very sharp lined and several close blends are resolved, e.g. the doublet structure of Mg II 4481Å is clearly seen (Fig. 3). The Mg II doublet is best fitted with no extra broadening (see Fig. 3, top panel), i.e. $v_{micro} \leq 3$ km/s. Alternatively, we can constrain the projected rotational velocity (see Fig. 3, bottom panel), an upper limit of $v_{rot} \sin i \leq 5$ km/s was adopted. Microturbulent and projected rotational velocities can also be constrained from unblended lines such as Si III 4552, 4567Å although the limits are not as strict ($v_{micro} \leq 5$ km/s, $v_{rot} \sin i \leq 10$ km/s) as those derived from the Mg II doublet. We adopt $v_{micro}=0$ km/s. An increase to 5 km/s translates into small systematic abundance uncertainties of 0.05dex for most ions. A temperature uncertainty of $\Delta T_{eff}=1000$ K translates into abundance uncertainties of less than 0.1 dex. Hence systematic errors are smaller for most ions than the statistical errors. The resulting abundances are listed in Table 2 and plotted in Fig. 6.

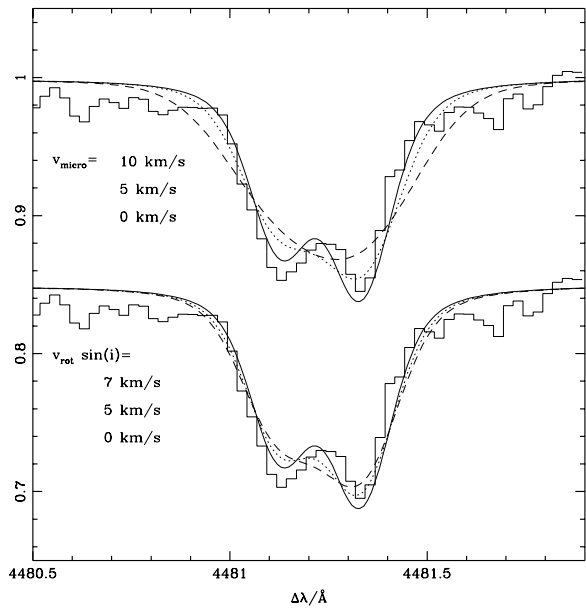


Fig. 3. Fit of the Mg II doublet for microturbulent velocities (top) of $v_{micro}=0$ (dotted), and 10 km/s (dashed) and projected rotational velocities (bottom) of $v_{rot} \sin i=0$, 5 (dotted), and 7 km/s (dashed)

3.2. KPD 2109+4401

As in the case of PG 1605+072 (paper I), He II 4686Å can be measured in the spectrum of KPD 2109+4401 allowing

Table 3. Atmospheric parameters for KPD 2109+4401 from different methods, see text

method	T_{eff} [K]	$\log g$	$\log \frac{n_{\text{He}}}{n_{\text{H}}}$
Billères et al. (1998)	31 200	5.84	
LTE: H+He [M/H]=0.0	31 200	5.77	-2.22
LTE: H+He [M/H]=-2.0	31 400	5.79	-2.31
LTE: He	32 400	5.81	-2.13
NLTE: H+He	31 200	5.69	-2.30
NLTE: He	32 500	5.73	-2.18
adopted	$31\,800 \pm 600$	5.76 ± 0.05	-2.23 ± 0.1

Table 4. Metal abundances for KPD 2109+4401 compared to solar composition. n is the number of spectral lines per ion.

ion	n	$\log \epsilon$	[M/H]
C III	-	<6.3	< -2.3
N II	2	7.26 ± 0.30	-0.69
N III	2	7.23 ± 0.03	-0.72
O II	-	<6.6	< -2.3
Ne II	-	<6.5	< -1.2
Mg II	-	<5.9	< -1.6
Al III	-	<5.3	< -1.1
Si III	-	<5.4	< -2.1
Si IV	-	<5.4	< -2.1
S III	2	6.50 ± 0.02	-0.66
Fe III	12	7.63 ± 0.21	+0.21

the helium ionization equilibrium to be exploited as well as Saffer's procedure. Both methods give parameters in reasonable agreement (see Table 3) and the averaged numbers ($T_{\text{eff}}=31\,800\text{K}$, $\log g=5.79$ $\log(\text{He/H})=-2.22$) were adopted for KPD 2109+4401. The line profiles calculated from this model reproduces the observed spectrum well (see Fig.4). The derived T_{eff} and $\log g$ are also in good agreement with the results from low resolution spectroscopy (Billères et al., 1998). Nitrogen is also present in two stages of ionization (N II and N III) and the effective temperature derived from its ionization equilibrium is in perfect agreement with the results from Balmer and helium line fitting.

Helium is depleted by a factor of 17 with respect to the sun.

From metal line profile fitting, as described for Feige 48, the projected rotational velocity of KPD 2109+4401 is constrained by our spectra to $v \sin i \leq 10\text{ km/s}$. The microturbulent velocity is constrained to $v_{\text{micro}} \leq 5\text{ km/s}$. Again we adopted $v_{\text{micro}}=0\text{ km/s}$ for further analysis.

Abundances of nitrogen, sulfur and iron were derived from the equivalent widths of their spectral lines. Upper limits for the abundances of carbon, oxygen, neon, magnesium, aluminium, and silicon were derived from the absence of the presumably strongest lines of those ions.

The resulting abundances are listed in Table 4 and plotted in Fig. 6.

Table 5. Atmospheric parameters for PG 1219+534 from different methods, see text

method	T_{eff} [K]	$\log g$	$\log \frac{n_{\text{He}}}{n_{\text{H}}}$
Koen et al. (1999)	$32\,800 \pm 300$	5.76 ± 0.04	-
LTE: H+He [M/H]=0.0	33 200	5.93	-1.60
LTE: H+He [M/H]=-2.0	33 200	5.95	-1.62
LTE: He	35 200	6.03	-1.41
NLTE: H+He	33 300	5.85	-1.56
NLTE: He	35 400	5.87	-1.38
adopted (see text)	$34\,300^{+2000}_{-1000}$	5.95 ± 0.1	-1.5 ± 0.1

Table 6. Metal abundances for PG 1219+534 compared to solar composition. n is the number of spectral lines per ion.

ion	n	$\log \epsilon$	[M/H]
C III	-	<6.6	< -2.0
N II	7	7.79 ± 0.08	-0.16
N III	5	7.79 ± 0.16	-0.16
O II	-	<7.0	< -1.9
Ne II	-	<6.7	< -1.0
Mg II	-	<6.2	< -1.3
Al III	-	<5.7	< -0.7
Si IV	-	<5.6	< -1.9
S III	2	6.86 ± 0.06	-0.30
Fe III	2	7.56 ± 0.16	+0.13

Fontaine (1999, priv. comm.) obtained an improved light curve of KPD 2109+4401 and detected some structure in the Fourier spectrum, in particular, a symmetric quintuplet, which may be due to rotational splitting. A rotational period of about 6.6 days (or longer if not all the components of an n-tuplet are seen) has been inferred. Assuming a mass of $0.5M_{\odot}$ we derive a radius of $0.16R_{\odot}$ from its gravity, which results in a rotational velocity of 1.2 km/s, too small to be detected in our HIRES spectra.

3.3. PG 1219+534

As already pointed out by Koen et al. (1999) the helium lines are stronger than in most other sdB stars. He II 4686Å is detected allowing the He ionization equilibrium to be used as a temperature indicator. T_{eff} and $\log g$ derived with Saffer's procedure agree well with results from low resolution spectroscopy (Koen et al., 1999). However, unlike PG 1605+072 and KPD 2109+4401, the helium ionization equilibrium and Saffer's procedure yield discrepant results (see Table 5): $T_{\text{eff}}=33\,200\text{K}$, $\log g=5.93$, $\log(\text{He/H})=-1.60$ (Saffer's procedure, Fig. 5, top panel) and $T_{\text{eff}}=35\,200\text{K}$, $\log g=6.03$, $\log(\text{He/H})=-1.41$ (He ionization equilibrium, Fig. 5, bottom panel). At the lower T_{eff} the Balmer lines are well matched throughout the entire profile, whereas for He II 4686Å there is a significant mismatch (see Fig. 5, top panel). At the higher T_{eff} He II 4686Å is well reproduced, but the Balmer line cores

Fig. 4. Balmer and He line profile fits for KPD 2109+4401 of the HIRES spectrum.

are not reproduced at all (see Fig. 5, bottom panel). The line cores of He I 4026Å and 4471Å cannot be reproduced by either model. Despite of its high gravity PG 1219+534 has an unusually high helium abundance, i.e. helium is deficient by a factor of 2 to 5, only.

Besides the Balmer and the helium lines, metal lines of N II, N III, S III and Fe III are present. The ionization equilibrium of nitrogen (7 N II and 5 N III lines) can be used to determine the effective temperature, which requires the effective temperature to be as high as $T_{\text{eff}}=36800\text{K}$. At the low T_{eff} indicated by the Balmer line fit, the nitrogen abundance derived from N II lines differs from that derived from N III lines by almost 1 dex.

The abundances were calculated from the model most consistent with the nitrogen ionization equilibrium and results are listed in Table 6 and plotted in Fig. 6. The uncertainty in T_{eff} was taken into account when we estimated the upper limits for carbon, oxygen, neon, magnesium, aluminium and silicon from the absence of their presumably strongest lines.

Since the metal lines are very sharp we can constrain either the microturbulent velocity or the projected rotational velocity as demonstrated for Feige 48. Due to the weakness of the lines the limits are not as tight as for Feige 48: $v_{\text{micro}} \leq 5\text{ km/s}$, $v \sin i \leq 10\text{ km/s}$.

4. Discussion

We have determined atmospheric parameters (T_{eff} , $\log g$, He/H), metal abundances and projected rotation velocities from time averaged, high resolution spectra for four pulsating sdB stars (Paper I, this paper). The effective temperatures and gravities (see Fig. 1) confirm that KPD 2109+4401, PG 1219+534 and Feige 48 are bona-fide extended horizontal branch stars, the latter being on the terminal EHB line, whereas the gravity of PG 1605+072 is too low to be consistent with an EHB nature and might indicate a post- EHB evolutionary status for this star.

4.1. Atmospheric parameters

Using line blanketed LTE model atmospheres for solar and metal poor composition ([M/H]=-2.0) as well as line blanketed zero metalicity NLTE model atmospheres we found that

- metalicity effects are small.
- NLTE effects are unimportant for the temperature determination.
- there is an offset between gravities determined from the NLTE grid and the LTE grid. The NLTE gravities are slightly lower, by up to 0.1 dex.

A careful investigation of several temperature indicators, i.e. line profile fitting using Saffer's procedure, the ionization equilibria of helium, nitrogen and silicon gave consistent re-

Fig. 5. Top: Balmer and He line profile fits for PG 1219+534 of the HIRES spectrum. Note the mismatch of the He II 4686Å line profile and the cores of He I 4026Å and 4471Å.
Bottom: He line profile fits for PG 1219+534 of the HIRES spectrum to determine T_{eff} and $\log(\text{He}/\text{H})$ simultaneously, $\log g$ is adjusted to match the Balmer line wings. Note the mismatch of the cores of the Balmer lines and of He I 4026Å and 4471Å.

sults for Feige 48, KPD2109+4401 and PG 1605+072 (paper I). However, for PG 1219+534 a considerably higher effective temperature was derived from the ionization equilibria of nitrogen (36 800 K) and helium (34 400 K) than from the line profile fitting (Saffer's method, 33 200 K). What causes these discrepant results? NLTE effects might be considered. However, our NLTE calculations show that this is not the case for helium. For nitrogen such calculations are beyond the scope of this paper. In view of the consistent results for the other stars, NLTE effects for the N ionization equilibrium in PG 1219+534 appear unlikely.

PG 1219+534 has the highest He abundance and the shortest pulsation period of our programme stars. Hence the discrepancy could be related to these properties. Since the helium lines are stronger than in the other programme stars, line broadening is more important for the He I lines in the spectrum of PG 1219+534. We used tabulations of Barnard et al. (1969), Shamey (1969), Barnard et al. (1974, 1975) and Griem (1974) to compute the He I line profiles. New calculations have become available recently (Beauchamp et al., 1997). However, these tables are tailored for the use in white dwarf atmospheres and cannot be used for sdB stars because they do not extend to the significantly lower densities in the outer layers of sdB atmospheres. An extension of Beauchamp et al.'s tables would be useful for the sdB star line profile synthesis. For He II lines we used the tabulations of Schöning & Butler (1989).

Due to diffusion the helium distribution in the atmospheres could be inhomogeneous. If helium accumulates in the deeper atmospheric layers, the predicted He I line profiles, however, would be even broader and shallower, increasing the discrepancy with observations. A vertical stratification of helium, therefore, appears to be unlikely.

On the other hand the short pulsational periods ($P=128.1\text{ s} \dots 148.8\text{ s}$) observed for PG 1219+534 might indicate that the model assumption of hydrostatic equilibrium does no longer hold for the outer layers of the atmosphere, where the cores of the Balmer and He I, 4026, 4471 Å lines are formed. In this case T_{eff} derived from the He and N ionization equilibria should be preferred since the relevant lines form in deeper atmospheric layers.

Since the origin for the discrepancy remains unclear we adopted weighted means for the atmospheric parameters and had to admit a larger error range for PG 1219+534 than for the other programme stars.

4.2. Abundances

The resulting abundances are plotted in Fig. 6 and compared to PG 1605+072 (paper I). Although KPD 2109+4401 and PG 1219+534 do not display C, O, Ne, Mg Al and Si lines, stringent upper limits have been derived from the absence of the presumably strongest lines of these species.

Helium is depleted in all programme stars. Its abundances ranges from 1/80 solar (Feige 48) to 1/3 solar (PG 1219+534).

From the interplay of gravitational settling and radiative levitation, an anticorrelation between helium abundance and

gravity might be suspected. However no such correlation exists. This has also been found previously from studies of much larger samples of non-variable sdB stars (e.g. Schulz et al., 1991, Fontaine & Chayer, 1997).

Like helium the metals are deficient with respect to the sun. Iron, however, is a notable exception, since it is solar to within the error limits in all programme stars.

Large deficiencies of carbon, oxygen and silicon of up to 2 dex or more (KPD 2109+4401) have been found, whereas nitrogen and sulfur are only mildly deficient. In PG 1219+534 nitrogen is even almost solar. Large deficiencies of carbon and silicon as well as near solar nitrogen abundances have been reported for several non-variable sdB stars from high resolution UV spectroscopy (e.g. Heber et al. 1984b, Lamontagne et al. 1985, 1987, see Heber, 1998 for a review).

It is worthwhile to note that the abundances of C, O, Ne, Mg, Al and Si in the high gravity programme stars KPD 2109+4401 and PG 1219+534 are considerably lower than in the lower gravity stars PG 1605+072 and Feige 48 (see Fig. 6) which may point to the (selective) action of diffusion, i.e. an interplay between gravitational settling and radiative levitation. It is, however, puzzling that iron is solar irrespective of the stellar gravity.

Recently, Ohl et al. (2000) analysed the far UV spectrum of PG 0749+658, a sdB star somewhat cooler than our programme stars, obtained with the FUSE satellite and found solar abundances for several iron group elements. PG 0749+658 shares the mild depletion of nitrogen and sulfur with our programme stars. KPD 2109+4401 and PG 1219+4401 show a similarly strong deficiency of carbon and silicon as PG 0749+658 and several other non-variable sdBs (Baschek et al., 1982a,b; Lamontagne et al., 1985, 1987, Heber et al. 1984b).

However, until recently only a few diffusion calculations were available (e.g. Michaud et al. 1985). Photometric and spectroscopic observations of blue horizontal branch stars in globular clusters (Grudahl et al., 1999, Moehler et al., 1999, Behr et al., 1999a) stimulated calculations of atmospheric diffusion in atmospheres for such stars (Hui-Bon-Hoa et al., 2000), which are, however, considerably cooler than our programme stars. The predicted iron abundances are even larger than the observed ones.

For the sdB star PG 0749+658, Ohl et al. (2000) calculated equilibrium abundances within the framework of the radiative levitation theory and were able to reproduce the observed abundances of carbon, sulfur and iron, but predicted higher abundances for nitrogen and silicon and a much lower helium abundance than observed. Mass loss has frequently been invoked to explain the discrepancy between observed and predicted helium abundances (Fontaine & Chayer, 1997). Unglaub & Bues (1998) carried out diffusion calculation for helium, carbon and nitrogen for a model of $T_{\text{eff}}=40\,000\text{ K}$, $\log g=6.0$ including mass loss processes. For mass loss rates less than $10^{-13} M_{\odot}/\text{yr}$ the predicted helium, carbon and nitrogen abundance are qualitatively consistent with the observation. For a quantitative comparison additional calculations at lower effective temperatures and gravities as well as for various mass loss rates are required.

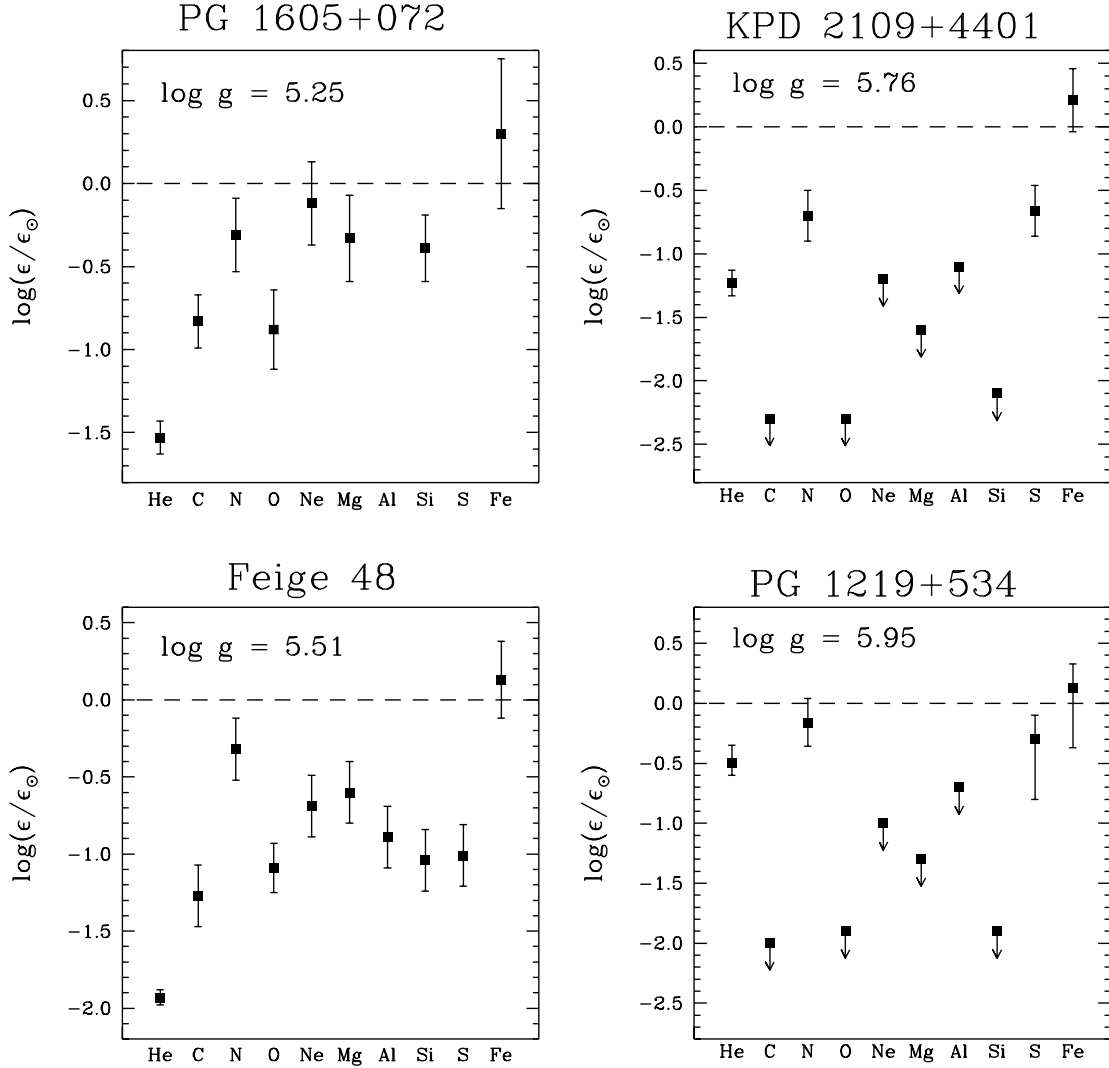


Fig. 6. Abundances of the programme stars relative to solar values

Finally, we point out that a solar surface iron abundance is consistent with the diffusion calculations of Charpinet et al. (1997) for the envelopes of pulsating sdB star models.

4.3. Rotation velocities

The spectral lines of PG 1605+072 are considerably broadened, which Heber et al. (1999) attributed to stellar rotation and derived $v \sin i = 39$ km/s, by fitting the strongest metal lines. Recently, O'Toole et al. (2000) performed time-series spectroscopy of PG 1605+072 and detected radial velocity variations at the same frequencies found from photometry with amplitudes up to 14 km/s at $H\beta$. Somewhat smaller velocity amplitudes were found for higher Balmer lines. The authors conclude that these velocity variations arise from the pulsations. Since part of the line broadening observed in the time averaged spectrum analysed in paper I may be due to ra-

dial velocity variations, the true projected rotational velocity is slightly smaller than $v \sin i = 39$ km/s. Feige 48, PG 1219+534 and KPD 2109+4401 are all very sharp-lined and we derived upper limits of $v \sin i < 5-10$ km/s (see above). This is consistent with time-series spectroscopy of KPD 2109+4401 (Jeffery & Pollaco, 2000) who measured radial velocity variations of 2 km/s, well below our detection limit. The same holds for any rotational broadening that has been inferred from the analysis of the light curve (Fontaine, 1999, priv. com., $v_{rot} \sin i = 1.2$ km/s or less).

The low projected rotational velocities of the pulsating sdB stars may be compared to the rotation velocities found for globular cluster horizontal branch stars, since sdB stars form the extremely hot end of the horizontal branch. Behr et al. (2000a,b) analysed Keck HIRES spectra of HB stars in the globular clusters M 13 and M 15 and found that a star's rotation appears to be related to its position along the horizontal branch. Stars hotter

Table 7. Radial velocities and equivalent widths of interstellar Ca II K derived by fitting the observed profile with three (PG 1219+534) or four Gaussian profiles.

Feige 48		KPD 2109+4401		PG 1219+534		PG 1605+072	
v km/s	W_λ mÅ	v km/s	W_λ mÅ	v km/s	W_λ mÅ	v km/s	W_λ mÅ
-55	63	-42	41	-57	78	-55	8
-38	38	-13	86	-28	70	-39	14
-17	53	3	31	-5	26	-18	96
5	12	11	11			0	68

than about 11 000 K were found to be rotating slowly ($v \sin i < 10$ km/s) whereas the cooler horizontal branch stars rotate more rapidly ($v \sin i \approx 40$ km/s for M 13) as previously observed by Peterson et al. (1995) for M 13. The low rotational velocities of our extreme horizontal branch stars are therefore consistent with the slow rotation derived for the hottest stars in M 13 and M 15. The rotating PG 1605+072 hence appears to be an exceptional case.

SdB stars are generally believed to evolve directly into white dwarfs which are mostly slow rotators as well (Heber et al., 1997, Koester et al., 1998).

5. Appendix: Interstellar Ca II K lines

Radial velocities and equivalent widths of interstellar Ca II K are derived by fitting the observed profile with three (PG 1219+534) or four Gaussian profiles. Results are listed in Table 7.

Acknowledgements. We thank Ralf Napiwotzki for many fruitful discussions. A travel grant to the W.M.Keck observatory by the Deutsche Forschungsgemeinschaft is gratefully acknowledged.

References

Barnard A.J., Cooper J., Shamey L.J., 1969, A&A 1,28
 Barnard A.J., Cooper J., Smith L.J., 1974, JQSRT 14, 1025
 Barnard A.J., Cooper J., Smith L.J., 1975, JQSRT 15,429
 Baschek B., Kudritzki R.P., Scholz M., Simon K.P., 1982a A&A 108, 387
 Baschek B., Höflich P., Scholz M., 1982b, A&A 112, 76
 Beauchamp A., Wesemael F., Bergeron P., 1997, ApJS 108, 559
 Behr B.B., Djorgovski S.G., Cohen J. G., et al., 1999, ApJ 517, L135
 Behr B.B., Djorgovski S.G., Cohen J. G., et al., 2000a, ApJ 528, 849
 Behr B.B., Cohen J. G., Mc Carthy J.K., 2000b, ApJ 528, 849
 Bergeron P., Saffer R. A., Liebert J., 1992, ApJ 394, 228
 Billères M., Fontaine G., Brassard P., et al., 1998, ApJ 494, L75
 Charpinet S., Fontaine G., Brassard P., Dorman B., 1996, ApJ 471, L106
 Charpinet S., Fontaine G., Brassard P., et al., 1997, ApJ 483, L123
 Cunto W., Mendoza C., 1992, Rev. Mex. Astron. Astrofis. 23, 107
 Dorman B., O'Connell, R.W., Rood R.T., 1995, ApJ 442, 105
 Edelmann H. 1998, Diploma Thesis, University of Erlangen-Nürnberg
 Ekberg J.O., 1993, A&AS 101, 1
 Fontaine G., Chayer P., 1997, *Proceedings of the Third Conference on Faint Blue Stars*, eds. A.G.D. Philip, J. Liebert and R.A. Saffer, Schenectady: L.Davis Press, p. 169
 Grundahl F., Catelan M., Landsman W.B., Stetson P.B., Andersen M.I., 1999 ApJ 524, 242
 Hagen H.-J., Groote D., Engels D., Reimers D., 1995, A&AS 111, 195
 Heber U., 1986, A&A 155, 33
 Heber U., 1998, in *Ultraviolet Astrophysics – Beyond the IUE Final Archive*, ESA SP-413, 195
 Heber U., Hunger K., Jonas G., Kudritzki R.P., 1984a, A&A 130, 119
 Heber U., Hamann W.-R., Hunger K., Kudritzki R.P., Simon K.P., Mendez R.H.: 1984b, A&A 136, 331
 Heber U., Napiwotzki R., Reid I.N., 1997, A&A 323, 819
 Heber U., Edelmann, H., Lemke M., Napiwotzki R., Engels D., 1999a, PASPC 169, 551
 Heber U., Reid I.N., Werner K., 1999b, A&A 348, L25
 Hui-Bon-Hoa A., LeBlanc F., Hauschildt P.H., 2000, ApJ 535, L45
 Jeffery C.S., Pollacco D., 2000, MNRAS in press
 Kawaler S., 1999, PASPC 169, 158
 Kilkenny D., Koen C., O'Donoghue D., Stobie R.S., 1997, MNRAS 285, 640
 Koen C., 1998, MNRAS 300, 567
 Koen C., O'Donoghue D., Pollacco D.L., Nitta A., 1998, MNRAS 300, 1105
 Koen C., O'Donoghue D., Pollacco D.L., Charpinet S., 1999, MNRAS 305, 28
 Koester D., Dreizler S., Weidemann V., Allard N.F., 1998, A&A 338, 612
 Kurucz, 1991, in: Crivellari L., Hubeny I., Hummer D.G. (eds.), *Stellar Atmospheres: Beyond Classical Methods*. Kluwer, Dordrecht, p.441
 Lamontagne R., Wesemael F., Fontaine G., Sion E.M. 1985, ApJ 299, 496
 Lamontagne R., Wesemael F., Fontaine G. 1987, ApJ 318, 844
 Ohl R.G., Chayer P., H.W. Moos, 2000, ApJ in press (astro-ph/0006235)
 Michaud G., Bergeron P., Wesemael F., Fontaine G., 1985, ApJ 299, 741
 Moehler S., Heber U., Lemke M., Napiwotzki R., 1998, A&A 339, 537
 Moehler S., Sweigart A.V., Landsman W.B. Heber U., Catelan M., 1999, A&A 346, L1
 Napiwotzki R., 1997, A&A 322, 256
 Østensen R., Solheim J.-E., Heber U., et al., 2000, A&A submitted
 O'Donoghue D., Koen C., Kilkenny D., Stobie R.S., 1999, Proc. of the 11th European Workshop on White Dwarfs, eds. J.E. Solheim & E.G. Meištas, ASP Conf. Series 169, 149
 O'Toole S.J., Bedding T.R., Kjeldsen H., et al., 2000, ApJ 537, L53
 Peterson R.C., Rood R.T., Crocker D.A., 1995, ApJ 453, 214
 Saffer R.A., Bergeron P., Koester D., Liebert J., 1994, ApJ 432, 351
 Schulz H., Heber U., Wegner G., 1991, PASP 103, 435
 Schöning T., Butler K., 1989, A&AS 78, 51
 Seaton M.J., 1987, J. Phys. B 20, 6363
 Silvotti R., Solheim J.-E., Gonzalez Perez, et al., 2000, A&A in press
 Unglaub K., Bues I., 1998, A&A 348, 75
 Vogt S.S., et al. 1994, SPIE 2198, 362
 Werner K., 1991, A&A 251, 147
 Werner K., Dreizler S., 1999, *Journal of Computational and Applied Mathematics*, Elsevier, 109, 65
 Wiese W.L., Smith M.W. & Miles B.M., 1969, *Atomic Transition Probabilities*, National Bureau of Standards, Washington

Wiese W., Fuhr J.R., Deters T.M. 1994, 1996, *J. Phys. Chem. Ref.*

 Data Monograph No. 7

Winget D.E., Nather R.E., Clemens J.C., et al., 1991, *ApJ* 378, 326

Zuckerman B., Reid I.N., 1998, *ApJ* 505, L143

